Contents lists available at SciOpen

Food Science and Human Wellness

journal homepage: https://www.sciopen.com/journal/2097-0765

China Food Publishing Co.

Infant feces-derived *Bifidobacterium breve* CCFM1078 inhibits the occurrence of rheumatoid cachexia by IRS1/PI3K/Akt signaling pathway

Bowen Li[a,b], Mengfan Ding[a,b], Chen Chi[a,b], Guoxun Shi[c,*], Xiaoming Liu[a,b], Jianxin Zhao[a,b,d], Paul Ross[d,e], Catherine Stanton[d,e,f], Wei Chen[a,b,g], Bo Yang[a,b,d,*]

[a] *State Key Laboratory of Food Science and Resources, Jiangnan University, Wuxi 214122, China*
[b] *School of Food Science and Technology, Jiangnan University, Wuxi 214122, China*
[c] *Department of Rheumatology, Jiangnan University Medical Center, Wuxi 214122, China*
[d] *International Joint Research Center for Probiotics & Gut Health, Jiangnan University, Wuxi 214122, China*
[e] *APC Microbiome Ireland, University College Cork, Cork T12 K8AF, Ireland*
[f] *Teagasc Food Research Centre, Moorepark, Fermoy P61 C996, Ireland*
[g] *National Engineering Research Center for Functional Food, Jiangnan University, Wuxi 214122, China*

ARTICLE INFO

Article history:
Received 23 January 2024
Received in revised form 12 April 2024
Accepted 24 May 2024

Keywords:
Bifidobacterium breve
Rheumatoid cachexia
Skeletal muscle
NF-κB pathway
IRS1/PI3K/Akt pathway
Gut microbiota

ABSTRACT

This study aimed to investigate the effects of infant feces-derived *Bifidobacterium breve* CCFM1078 on rheumatoid cachexia (RC). Twenty-four female Wistar rats were assigned to 3 groups: CON group (normal saline by gavage), CIA group (collagen-induced arthritis (CIA), normal saline by gavage), and CCFM1078 group (CIA, 3×10^9 CFU/(rat·day) *B. breve* CCFM1078 gavage). The results demonstrated that *B. breve* CCFM1078 not only improved skeletal muscle function in CIA rats, but also modulated the gut microbiota, skeletal muscle metabolism and hormone levels, reduced inflammation in the knee joint and skeletal muscles, decreased activity of the nuclear factor κB (NF-κB) inflammatory signaling pathway, enhanced the insulin receptor substrate 1 (IRS1)/phosphatidylinositol 3-kinase/protein kinase (PI3K/Akt) signaling pathway, promoted skeletal muscle differentiation, and maintained skeletal muscle fiber diameter, consequently slowing down the progression of RC. These findings suggested that *B. breve* CCFM1078 may have a beneficial role as part of a dietary intervention for RC, enhancing overall therapeutic effects.

1. Introduction

Rheumatoid cachexia (RC) is a common complication in patients with rheumatoid arthritis (RA)[1]. The main manifestations include muscle wasting and reduction, decreased muscle strength, muscle pain, and muscle stiffness. Cachexia is more common in patients with higher disease activity[2]. According to current data, there are 18 million people worldwide suffering from RA, and approximately 30%–40% of RA patients have cachexia[3]. The development of cachexia is influenced by various factors, including disruption of energy metabolism caused by chronic inflammation, decreased appetite, and increased protein degradation. RC can lead to overall physical weakness, limited mobility, increased susceptibility to infections, and delayed wound healing, severely affecting the life quality of the patients and disease prognosis. It has been shown that RC is highly prevalent in early-stage RA[2]. Early detection of this condition and the application of relevant treatments to improve inflammation and adjust the body's condition, along with dietary modifications, are of concern to food nutrition.

Skeletal muscle atrophy, as the main feature of RC, is associated with the differentiation and dysbiosis of gut microbiota[4]. A crosstalk and close metabolic interactions take place between the gut microbiota

* Corresponding author.
E-mail address: shiguoxun2003@163.com (G.X. Shi); bo.yang@jiangnan.edu.cn (B. Yang)
Peer review under responsibility of Beijing Academy of Food Sciences.

SciOpen Publishing services by Tsinghua University Press

http://doi.org/10.26599/FSHW.2024.9250323

composition-function and the muscle physiology and function. It has shown that in mice with muscle malnutrition, there is an increase in Gram-negative bacteria producing lipopolysaccharide (LPS) in the gut, a decrease in gut motility, damage to tight junctions, and an upregulation of the bacterial pro-inflammatory receptor Toll-like receptor 4 (TLR4)-MyD88 signaling in the muscles[5]. The gut microbiota is involved in influencing changes in insulin sensitivity that affect glucose absorption, adjusting changes in the exercise capacity of experimental animals[6]. In patients with inflammatory myopathies, there is an increase in the relative abundance of Prevotellaceae, while the relative abundance of certain butyric acid-producing bacteria such as *Pseudobutyrivibrio* and Lachnospiraceae show a significant decrease. However, after treatment with interleukin (IL)-2, the relative abundance of *Pseudobutyrivibrio*, Lachnospiraceae, and other bacteria tends to be recovered[7]. Therefore, regulating the diversity and composition of the gut microbiota through the gut microbiota may be a feasible approach for early dietary intervention in RC and RA.

According to the definition by the Food and Agriculture Organization (FAO) in 2002, probiotics are live microorganisms that, when ingested in sufficient amounts, provide health benefits to the host[8]. Taking probiotics may be the most widely used method for modulating the gut microbiota. It has shown that *Lactobacillus paracasei* PS23 can improve exercise-induced muscle damage and attenuate testosterone decline[9]. Oral administration of *L. rhamnosus* NR_113332.1 can improve skeletal muscle fiber regeneration effect in mice[10]. Additionally, supplementation with *L. rhamnosus* 100-23 and *L. gasseri* 311476 can reduce the expression of muscle atrophy markers Atrogin-1, MuRF1, and LC3 in the gastrocnemius and tibialis anterior muscles of leukemic cachexia mice[11].

Bifidobacterium breve CCFM1078 isolated from infant feces in Wuxi, China, has been found to have the ability to alleviate RA in our previous research. Its main effect lies in improving the intestinal barrier of CIA rats, increasing tight junction proteins expression in the intestines, and reducing the translocation of LPS[12]. Based on previous results, we hypothesize that *B. breve* CCFM1078 may have a beneficial effect on RC. The collagen-induced arthritis (CIA) rat model has been proven to be a suitable model for evaluating the pathogenesis of RC[13]. This study aimed to evaluate the impact of CCFM1078 on the occurrence and progression of RC in CIA rats and explore the potential mechanism by which it may alleviate RC. It helps to establish a theoretical foundation for the development of related dietary supplements for adjuvant therapy of RC.

2. Method

2.1 Animal experiment design

Twenty-four 5-week-old female Wistar rats were purchased from Charles River Ltd. (Zhejiang, China). Rats were divided into 3 groups, namely the control group (CON group), CIA group (CIA group), and *B. breve* CCFM1078 group (CCFM1078 group), with 8 rats in each group, after one week of adaptation. The test was conducted following the schematic in Fig. 1A. Gavage was initiated in the 2nd week of the experiment, with the CCFM1078 group receiving 3×10^9 CFU/(rat·day) of *B. breve* CCFM1078, while the CON and CIA groups received the same volume of saline. The method of inducing CIA referred to previous studies[12]. Briefly, on the first day of the 3rd week and the first day of the 4th week, the initial immunization and immune stimulation of CIA were performed by subcutaneous injection in the tail of the CIA group and the CCFM1078 group, while the CON group received an equal amount of saline by subcutaneous injection in the tail. During the final week of the study, measurements were taken for both rat paw thickness and arthritis scores. The scoring criteria for arthritis were adopted from our previous study[14]. All procedures used in animal experiments were examined and approved by Jiangnan University Experimental Animal Management and Animal Welfare Ethics Committee, and the 1964 Declaration of Helsinki and its subsequent modifications. Ethical review number is JN. No20220315W0880618[019].

2.2 Rat pull test

A rat pull test was performed before euthanizing rats. The instrument used for testing the pull force of the animal's claws was purchased from BIOSEB (Vitrolles, France). The test followed the instructions provided by the manufacturer. In summary, the rat's body was held slowly lower until the animal's claws caught the central area of the test grid. Along the direction of the sensor, the rat's tail was pulled horizontally until claws released the test grid. The maximum pulling force of the animal on the grid was displayed on the screen. Each animals tested 3 times and record the pulling force of each animal.

2.3 Sample collection

After the pull test, rat feces were collected. Then, the rats were anesthetized with isoflurane, and after the extraction of blood from the heart, they were euthanized by dislocating the cervical vertebrae. The left knee joint and skeletal muscle were dissected and soaked in a solution of polyformaldehyde fixative for the preservation of pathological sections.

The right knee joint and skeletal muscle, as well as the serum were stored at −80 ℃ for subsequent tests. The assay reagents employed in the experiments were listed in the Supplementary Materials.

2.4 Pathological sections and immunofluorescence

The pathological sections and immunofluorescence were conducted referring to previous research[12]. Briefly, joint and skeletal muscle tissues were underwent fixation with paraformaldehyde (extra decalcification is required for joint tissues), followed by dehydration, and embedding in paraffin blocks. The paraffin blocks were cut into 5 μm sections using an automated microtome. Afterward, staining or antibody incubation was performed. Finally, the fine structures were observed and analyzed either through a slide scanner Panoramic MIDI device (3D HISTECH, Budapest, Hungary) or a microscope. The relative expression levels of immunofluorescence were calculated using ImageJ.

2.5 Enzyme-linked immunosorbent assay (ELISA)

ELISA kits for rheumatoid factor (RF), C-reactive protein (CRP), anti-cyclic citrullinated peptide antibodies (anti-CCP), IL-6, tumor

necrosis factor-α (TNF-α), IL-17, muscle glycogen (MG), lactate, 11β-hydroxysteroid dehydrogenase 1 (11β-HSD1), 25(OH)D_3, myostatin (MSTN), Fbox-1, myoblast determination protein 1 (MyoD), albumin (ALB), and transforming growth factor beta 1 (TGF-β1) were purchased from Huijia Biotechnology Co., Ltd. (Xiamen, China) and were tested according to the instructions provided by the manufacturer. BCA assay kit (Waltham, MA, U.S.A.) was used to measure the protein concentration in tissue samples.

2.6 Fecal microbiota analysis

The method of analyzing the gut microbiota referred to previous report[15]. In brief, the FastDNA spin kit for feces (MP Biomedicals, CA, U.S.A.) was used to extract fecal DNA. The extracted fecal DNA was then subjected to polymerase chain reaction (PCR) amplification targeting the V3−V4 region of the 16S rRNA gene and the bifidobacterial *groEL* gene, followed by agarose gel electrophoresis to detect the amplified production and purification of the PCR products. Based on the purity of the products, samples of different volumes were mixed to obtain a DNA library with an equal concentration of DNA. Library construction and sequencing were then performed. The data obtained from sequencing were analyzed using QIIME2. The primer sequences used for V3−V4 region of the 16S rRNA gene and the bifidobacterial *groEL* gene were shown in Table S1.

2.7 Quantitative real-time PCR (qRT-PCR)

The method of qRT-PCR was performed according to the previously described[16]. In brief, total RNA was extracted from the tissues using the TRIzol method, quantified, and reverse transcribed into cDNA. The subsequent detection was performed using the cDNA. The primer sequences used for qRT-PCR were shown in Table S2.

2.8 Western blot

The Western blot method referred to a previous description[17]. β-Actin was used as a housekeeping gene. ImageJ software was used to analyze the grayscale of the bands.

2.9 Statistical analysis

The data were presented as the mean and standard deviation (mean ± SD). One-way analysis of variance (ANOVA) Duncan test and *t*-tests were used to determine whether significant differences existed between the groups. And the *P*-value below 0.05 indicated significant differences between the groups.

3. Results

3.1 Effects of B. breve CCFM1078 on the arthritis progression and pull force of CIA rats

After 3 weeks of the initial immunization, the body weight of the CON and CCFM1078 group was significantly higher than that of the CIA group ($P < 0.05$, Fig. 1B). There were significant differences among the 3 groups in terms of paw thickness and arthritis score ($P < 0.05$), with the CIA group showing the highest values and the CON group showing the lowest values (Figs. 1C and D). The pull force of rats in the CIA group was significantly lower than that of the CON group and CCFM1078 group ($P < 0.05$, Fig. 1E). There were significant differences among the 3 groups in terms of serum RF and serum anti-CCP ($P < 0.05$), with the highest values in the CIA group, the lowest values in the CON group, and the CCFM1078 group falling in between (Figs. 1F and H). The serum CRP level in the CIA group was significantly higher than that of CON and CCFM1078 groups ($P < 0.05$, Fig. 1G). From the images of rat paws, it can be observed that the paws of the CON group were not swollen, the paw pads of the CIA group were swollen and enlarged, and the paws of the CCFM1078 group showed only slight redness and swelling (Figs. 1I-K).

3.2 Effects of B. breve CCFM1078 on the pathological levels of knee joint and skeletal muscles in CIA rats

The HE stains in the knee joints showed that there was severe inflammatory infiltration and tissue morphology damage in the trabecular bone and synovium of the CIA group rats, while the CCFM1078 group had lower levels of trabecular bone inflammatory infiltration than the CIA group (Fig. 2A). Safranin-O and fast green staining were used to evaluate the changes in articular cartilage in CIA rats (Fig. 2B). The red part represented the cartilage. It can be observed that the thickness of the articular surface and subchondral cartilage layer of the CIA group were smaller than those of the CON group and CCFM1078 group. HE stains of skeletal muscle showed that, at the same magnification, the diameter of muscle fibers in the CIA group was smaller than that in the CON group and CCFM1078 group, while the diameter of muscle fibers in the CCFM1078 group was similar to that in the CON group (Fig. 2C). Masson staining of skeletal muscle showed that the CON group and CCFM1078 group had relatively more blue collagen fibers compared to the CIA group, and Masson staining also revealed the phenomenon of muscle atrophy in the CIA group, with smaller muscle fiber diameter compared to the CON group and CCFM1078 group (Fig. 3C).

3.3 Effects of B. breve CCFM1078 on the inflammation factors of knee joints in CIA rats

The knee joint immunofluorescence indicated that the relative expression of IL-6 in the CIA group was significantly higher than that in the CON group and CCFM1078 group ($P < 0.05$, Figs. 3A and B). There were significant differences in the relative expression of TNF-α among the three groups ($P < 0.05$, Figs. 3D and E), with the CCFM1078 group falling between the CIA group and CON group, and the CIA group having the highest relative expression. The results of ELISA were similar to those of immunofluorescence. There were significant differences in the levels of IL-6 among the three knee joint groups ($P < 0.05$, Fig. 3C). The levels of TNF-α in the CON group and CCFM1078 group knee joints were significantly lower than those in the CIA group ($P < 0.05$, Fig. 3F).

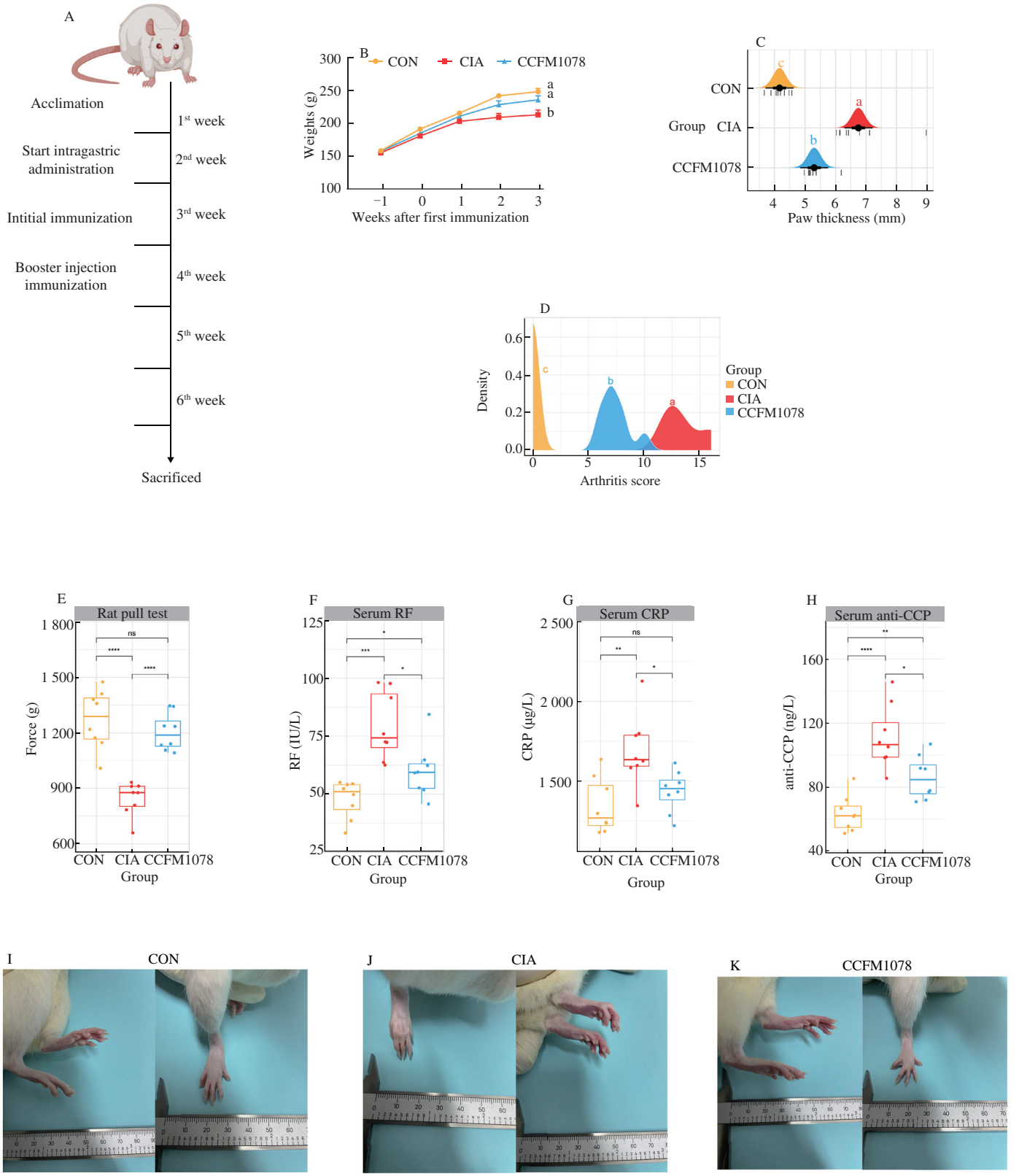

Fig. 1 Effects of *B. breve* CCFM1078 on the development of RC in CIA rats. (A) Experimental design, (B) rats body weight, (C) rat paw thickness, (D) rat arthritis score, (E) rat pull force, (F) serum RF, (G) serum CRP, (H) serum anti-CCP, (I) CON group rat claws, (J) CIA group rat claws, (K) CCFM1078 group rat claws. RF, rheumatoid factor; CRP, C reactive protein; anti-CCP, anti-cyclic peptide containing citrulline. The completely different letters between each group represent significant differences, $^{*}P < 0.05$, $^{**}P < 0.01$, $^{***}P < 0.001$, $^{****}P < 0.000\ 1$; ns, no significant.

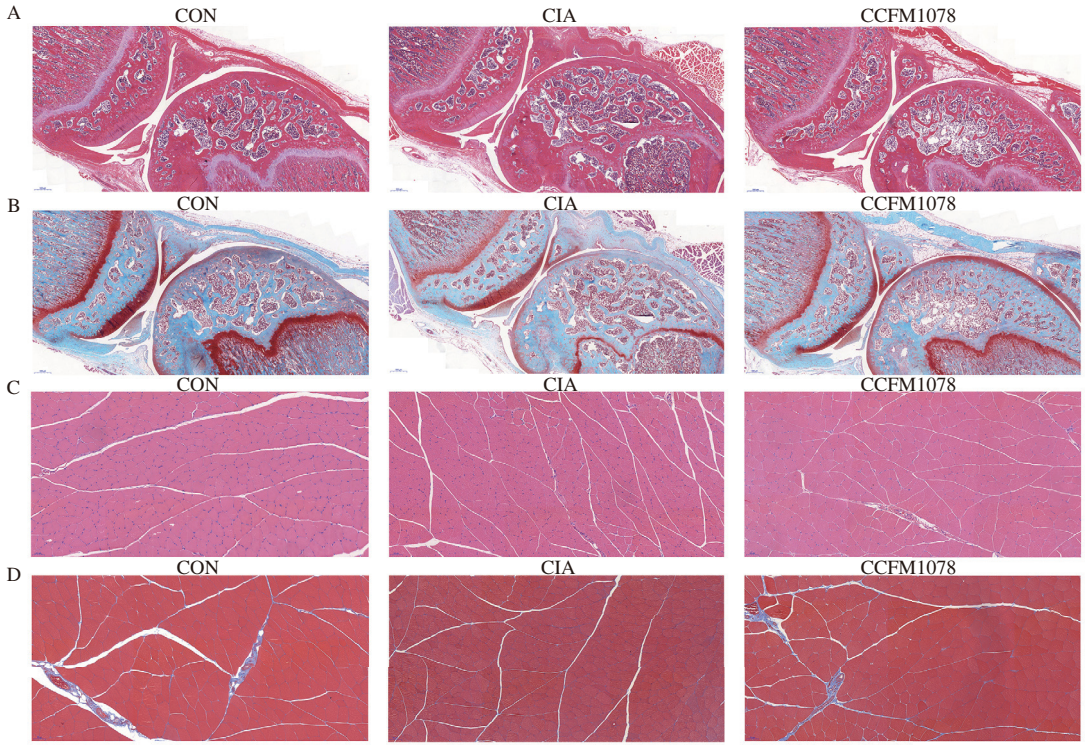

Fig. 2 Effects of *B. breve* CCFM1078 on pathological structure of knee joint and skeletal muscle in CIA rats. (A) HE stains of the knee joint, magnification: 2.5×, (B) safranin-O and fast green staining of the knee joint, magnification: 2.5×, (C) HE stains of skeletal muscle, magnification: 18×, (D) Masson staining of skeletal muscle, magnification: 18×.

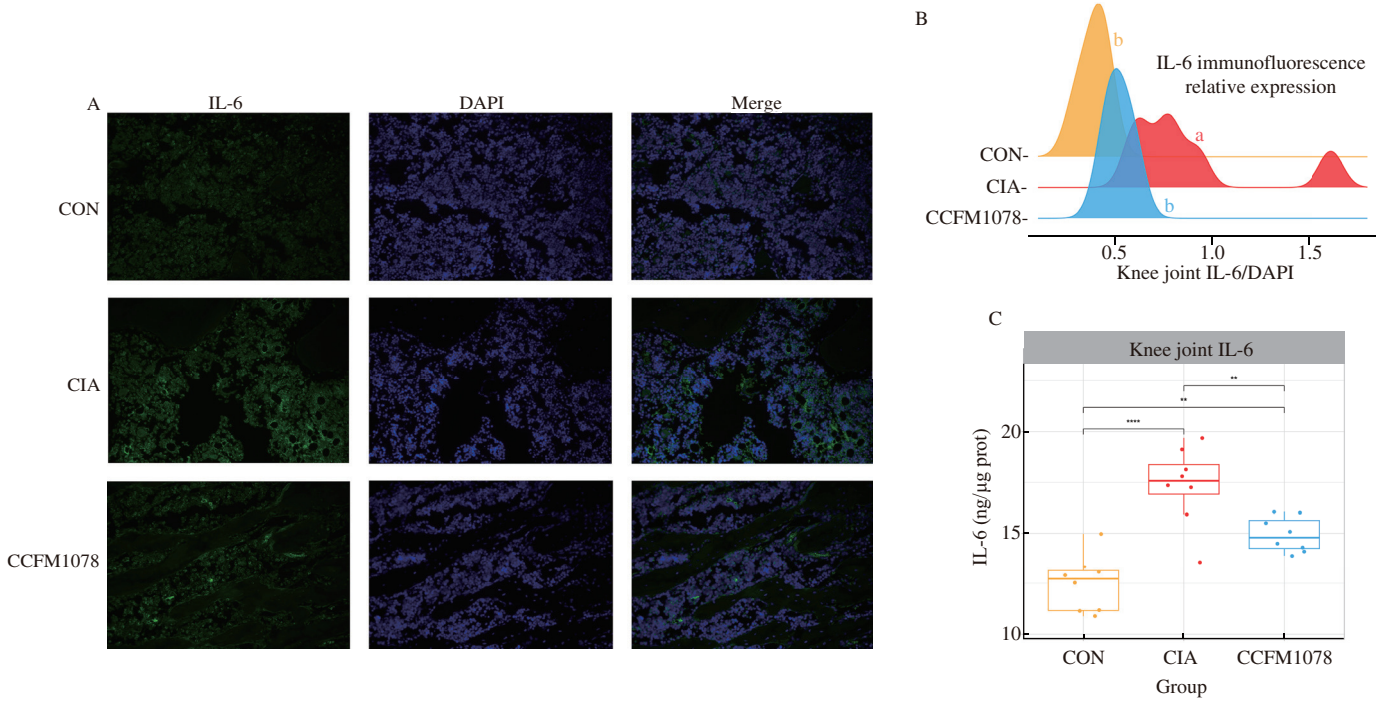

Fig. 3 Effects of *B. breve* CCFM1078 on inflammatory factors in knee joints of CIA rats.(A) Knee joint IL-6 immunofluorescence, magnification: 200×, (B) immunofluorescence relative expression of knee joint IL-6 (IL-6/DAPI), (C) IL-6 content in knee joint, (D) knee joint TNF-α immunofluorescence, magnification: 200×, (E) immunofluorescence relative expression of knee joint TNF-α (TNF-α/DAPI), (F) TNF-α content in knee joint. The completely different letters between each group represented significant differences, $^{*}P < 0.05$, $^{**}P < 0.01$, $^{***}P < 0.001$, $^{****}P < 0.000\ 1$; ns, no significant.

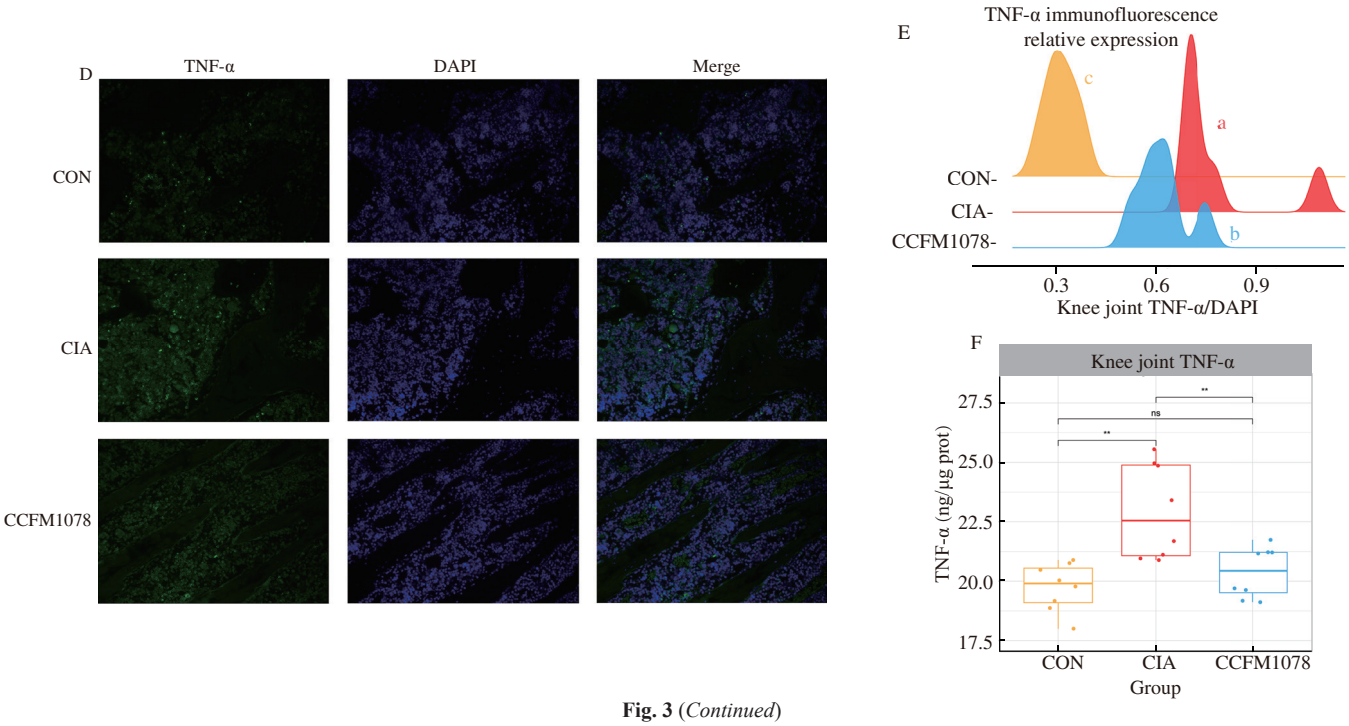

Fig. 3 (*Continued*)

3.4 Effects of B. breve CCFM1078 on skeletal muscle inflammation factors and markers related to muscle differentiation and atrophy

The immunofluorescence and ELISA for skeletal muscle tissue indicated that the relative expression levels of IL-6, TNF-α, and IL-17 in the CON and CCFM1078 groups were significantly lower than those in the CIA group ($P < 0.05$, Figs. 4A-B, D, F-G, H, J-K, and L). At the metabolic level of the skeletal muscle, the MG content in the CON and CCFM1078 groups were significantly higher than that in the CIA group, and lactate in the CON and CCFM1078 groups was significantly lower than that in the CIA group ($P < 0.05$, Fig. 4C). In terms of hormonal indicators in the skeletal muscle, the level of 11β-HSD1 in the CON group was significantly lower than that in the CIA group; although the level in the CCFM1078 group was lower than that in the CIA group, there was no significant difference between the two groups. The levels of 25(OH)D_3 in the skeletal muscles of the CON and CCFM1078 groups were significantly higher than those in the CIA group ($P < 0.05$, Fig. 4E). Regarding muscle atrophy and differentiation factors, the levels of MSTN and Fbox-1 in the skeletal muscles of the CON and CCFM1078 groups were significantly lower than those in the CIA group; the level of MyoD in the skeletal muscles of the CON and CCFM1078 groups was significantly higher than that in the CIA group ($P < 0.05$, Fig. 4I). Additionally, the level of ALB in the serum of the CON and CCFM1078 groups was significantly higher than that in the CIA group ($P < 0.05$, Fig. 4M).

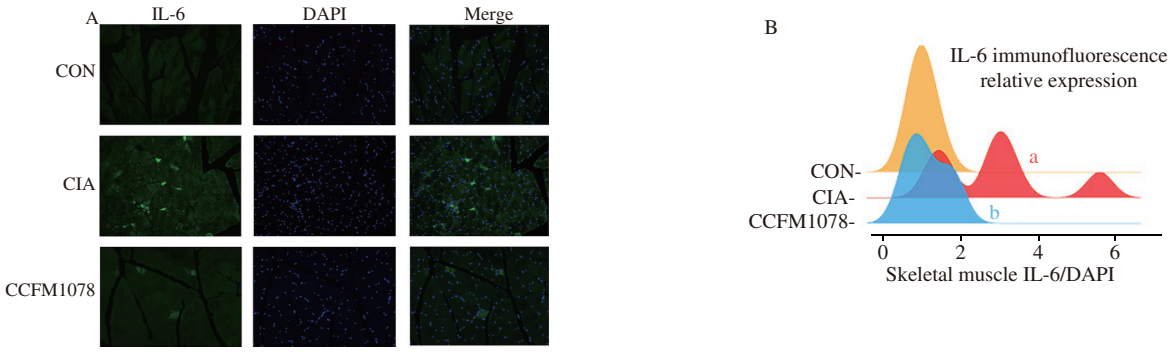

Fig. 4 Effects of *B. breve* CCFM1078 on skeletal muscle inflammatory factors and biomarkers of RC. (A) Skeletal muscle IL-6 immunofluorescence, magnification: 200×. (B) Immunofluorescence relative expression of skeletal muscle IL-6 (IL-6/DAPI). (C) Skeletal muscle MG and lactate. (D) IL-6 content in skeletal muscle. (E) Skeletal muscle 11β-HSD1 and 25(OH)D_3. (F) Skeletal muscle TNF-α immunofluorescence, magnification: 200×. (G) Immunofluorescence relative expression of skeletal muscle TNF-α (TNF-α/DAPI). (H) TNF-α content in skeletal muscle. (I) Skeletal muscle MSTN, Fbox-1, MyoD. (J) Skeletal muscle IL-17 immunofluorescence, magnification: 200×. (K) Immunofluorescence relative expression of skeletal muscle IL-17 (IL-17/DAPI). (L) IL-17 content in skeletal muscle. (M) Serum ALB. The completely different letters between each group represented significant differences. $^{*}P < 0.05$, $^{**}P < 0.01$, $^{***}P < 0.001$, $^{****}P < 0.000\ 1$; ns, no significant.

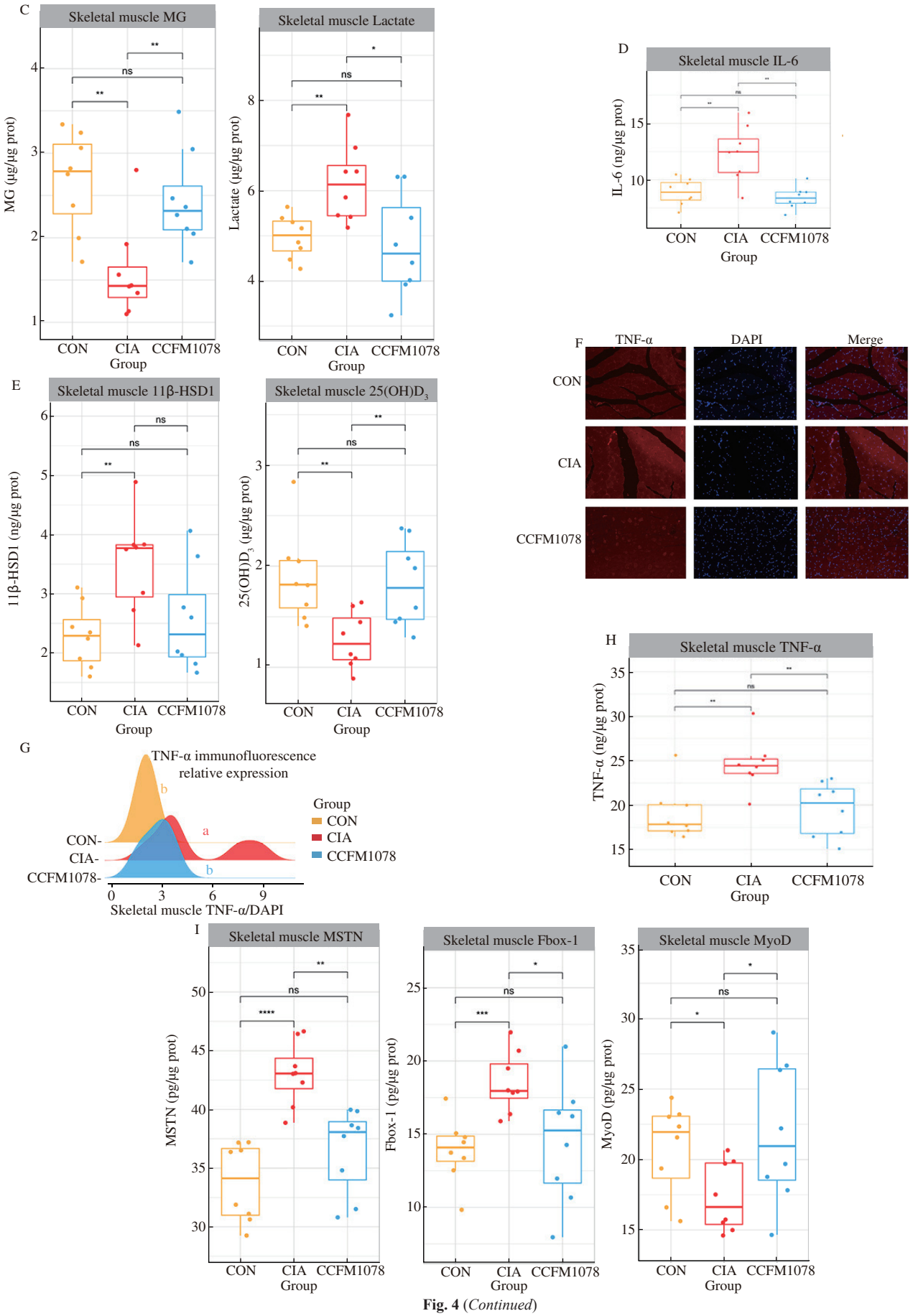

Fig. 4 (*Continued*)

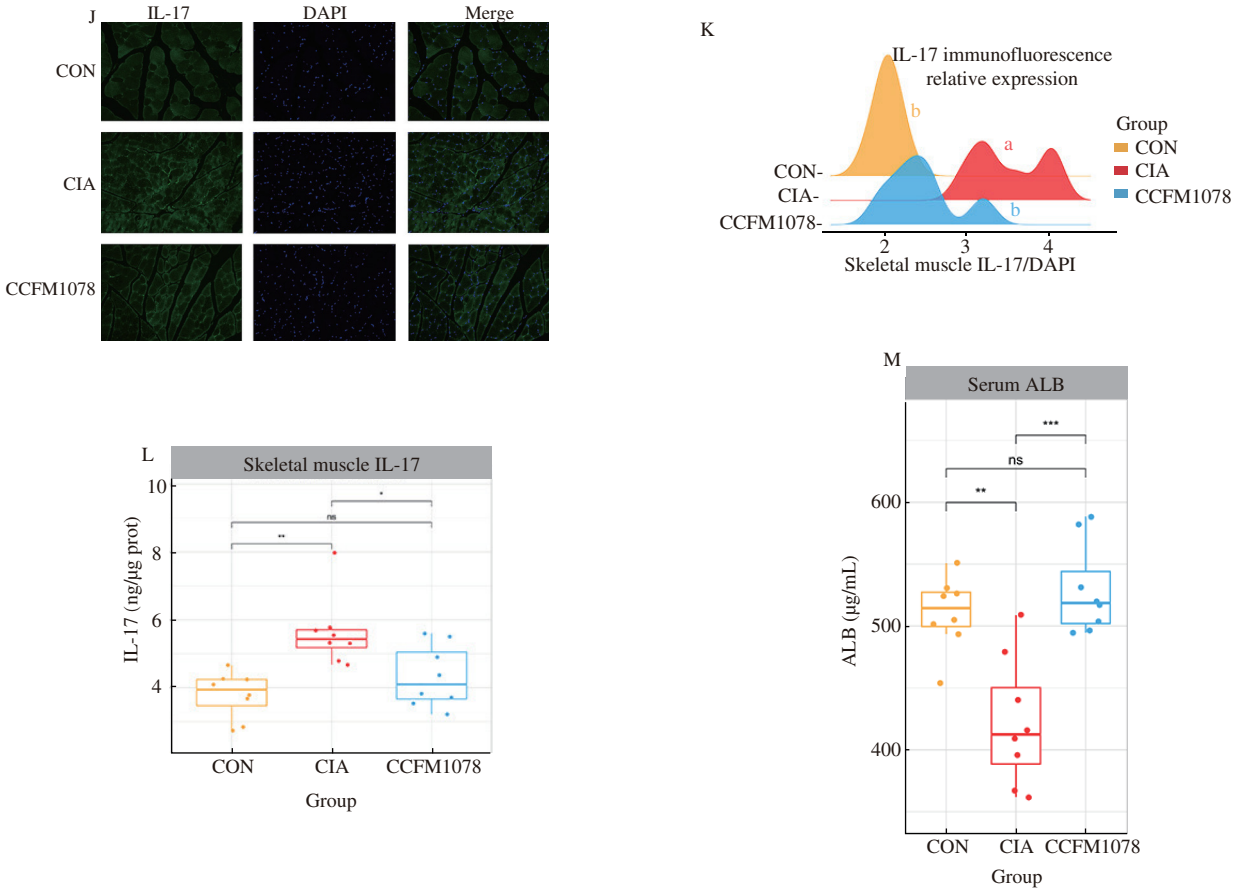

Fig. 4 (*Continued*)

3.5 Effects of B. breve CCFM1078 on fecal microbiota and Bifidobacteria in CIA rats

The 16S rRNA gene sequencing results showed that *B. breve* CCFM1078 did not alter the *α*-diversity of gut microbiota in CIA rats but had an impact on the beta diversity of gut microbiota ($P = 0.001$, Figs. 5A-D). At the genus level, the top 30 most relative abundance genera were displayed in Fig. 5H. Among all sequenced genera, there were three unique genera in the CON group, 16 unique genera in the CIA group, and seven unique genera in the CCFM1078 group, with a total of 113 genera shared among the three groups. The relative abundance of *Akkermansia* in the CON group was significantly higher than that in the CIA group ($P < 0.05$). The relative abundance of *Alistipes* in the CIA group was significantly higher than that in the CON group and CCFM1078 group ($P < 0.05$). The relative abundance of *Alloprevotella* and Ruminococcaceae UCG-010 in the CIA group was significantly higher than that in the CON group ($P < 0.05$). The relative abundance of *Bifidobacterium* in the CCFM1078 group was significantly higher than that in the CON group and CIA group ($P < 0.05$). The relative abundance of *Clostridium sensu stricto* 1 and *Ruminococcus* 1 in the CCFM1078 group was significantly higher than that in the CON group ($P < 0.05$). The relative abundance of *Lachnocostridium*, Lachnospiraceae NK4A136 group, and Roseburia in the CON group and CIA group was significantly higher than that in the CCFM1078 group ($P < 0.05$). The relative abundance of *Turicibacter* in the CON group and CCFM1078 group was significantly higher than that in the CIA group ($P < 0.05$, Figs. 5H and J).

For *Bifidobacterium*, *B. breve* CCFM1078 significantly altered the alpha diversity of the bifidobacterial community (Figs. 5E-G), particularly the Shannon index ($P < 0.05$, Fig. 5F). *B. breve* CCFM1078 also significantly affected the beta diversity of gut microbiota ($P = 0.001$, Fig. 5L). The relative abundance of *B. breve* in the CCFM1078 group was significantly higher than that in the CON group and CIA group ($P < 0.05$). The relative abundance of *B. longum* subsp. *infantis* and *B. longum* subsp. *longum* in the CON group was significantly higher than that in the CIA group and CCFM1078 group ($P < 0.05$). In addition, the relative abundance of *B. pseudolongum* in the CCFM1078 group was significantly lower than that in the CIA group ($P < 0.05$, Figs. 5K and M).

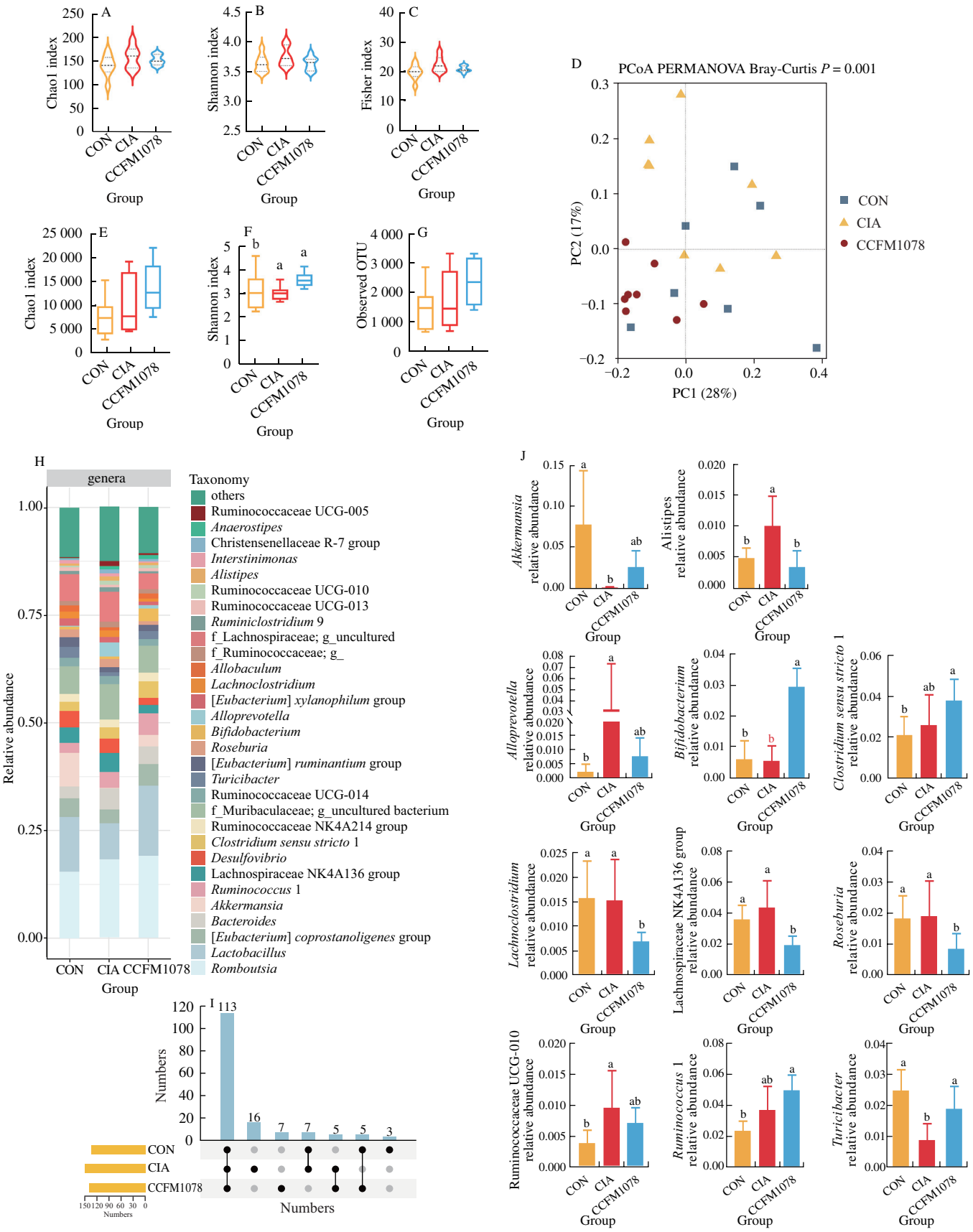

Fig. 5 Regulation of *B. breve* CCFM1078 on the gut microbiota structure of CIA rats. (A) Chao1 index. (B) Shannon index. (C) Fish index. (D) Beta diversity. (E) Bifidobacterial Chao1 index. (F) Bifidobacterial Shannon index. (G) Bifidobacterial observed OTU. (H) Top 30 genera stack plot. (I) Upset plot. (J) Relative abundance of differential bacteria at the genus level. (K) Bifidobacterial stack plot. (L) Bifidobacterial beta diversity. (M) Relative abundance of differential *Bifidobacterium* species levels. The completely different letters between each group represented significant differences, $P < 0.05$.

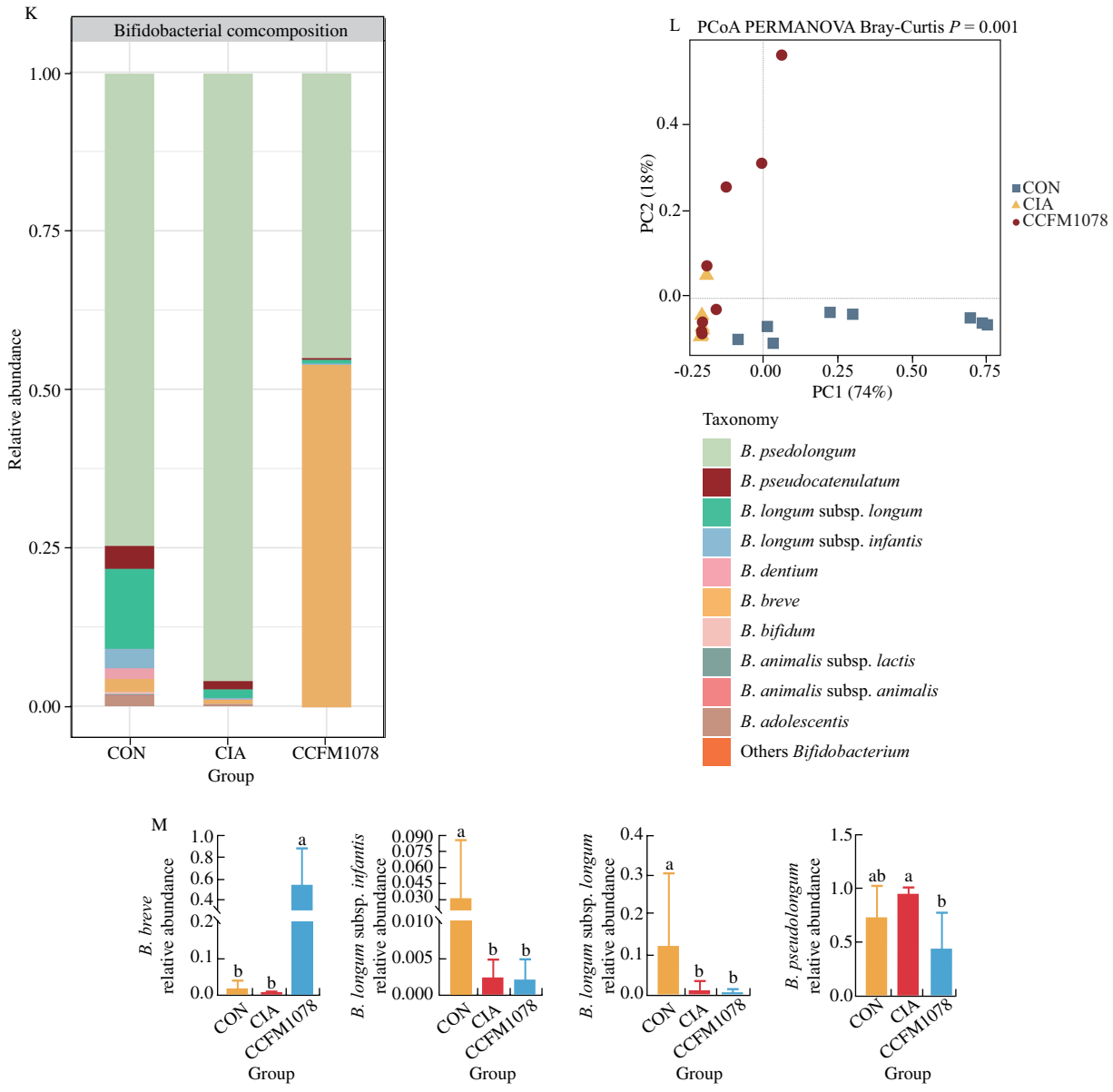

Fig. 5 (*Continued*)

3.6 Effects of B. breve CCFM1078 on the expression of NF-κB inflammation pathway and muscle atrophy-related genes and proteins in skeletal muscles in CIA rats

In terms of gene expression, there were significant differences in the relative expression levels of *IKKα* and *STAT3* among the three groups, with the highest relative expression level in the CIA group and the lowest in the CON group ($P < 0.05$, Fig. 6B). The relative expression levels of NF-κB and Fbox-1 in the CON and CCFM1078 groups were significantly lower than those in the CIA group ($P < 0.05$, Fig. 6B). The expression level of *MuRF1* in the CIA group was significantly higher than in the CON group ($P < 0.05$, Fig. 6B). In terms of protein expression, there were significant differences in the relative expression levels of *p-IKKα* and *p-STAT3* among the three groups ($P < 0.05$, Figs. 6C and E). The relative expression level of *p-NF-κB* in the CON group and the CCFM1078 group was significantly lower than in the CIA group ($P < 0.05$, Fig. 6D).

3.7 Effects of B. breve CCFM1078 on the IRS1/PI3K/AKT pathway and muscle differentiation-related gene proteins in skeletal muscles in CIA rats

The immunofluorescence relative expression levels of TGF-β1 and Glut4 in skeletal muscle of the CON group and the CCFM1078 group were significantly higher than those of the CIA group ($P < 0.05$, Figs. 7A-B, E-F). The ELISA results showed that the content of TGF-β1 in the skeletal muscle of the CON group and the CCFM1078 group was significantly higher than that of the CIA group ($P < 0.05$, Fig. 7D), which was consistent with the results of immunofluorescence. At the gene level, the relative expression levels of *IGF1*, *TGF-β1*, *IRS1*, *PI3K*, *Akt*, *Glut4*, *MyoD*, *MyoG*, and *GSK3β* in the CON group and the CCFM1078 group were significantly higher than those of the CIA group ($P < 0.05$, Figs. 7G and H), and the relative expression levels of *IRS1* and *Akt* in the CON group were significantly higher than those in the CCFM1078 group. In terms of non-coding RNA, there were significant differences in

the expression of H19 among the three groups ($P < 0.05$), and the relative expression levels of miR-29b-3p in the CON group and the CCFM1078 group were significantly lower than those in the CIA group ($P < 0.05$, Fig. 7I). In terms of protein expression, the relative expression levels of p-IRS1 and p-PI3K in the CON group and the CCFM1078 group were significantly higher than those in the CIA group ($P < 0.05$, Figs. 7C, J, and K). In addition, there were significant differences in the relative expression levels of IGF1R and Glut4 among the three groups, with the CCFM1078 group having the highest expression and the CIA group having the lowest expression ($P < 0.05$, Figs. 7C, L, and N). The relative expression level of p-Akt in the CCFM1078 group was significantly higher than that in the CIA group ($P < 0.05$, Figs. 7C and M). There were significant differences in the relative expression levels of MyoG among the three groups, with the CON group having the highest expression and the CIA group having the lowest expression ($P < 0.05$, Figs. 7C and O).

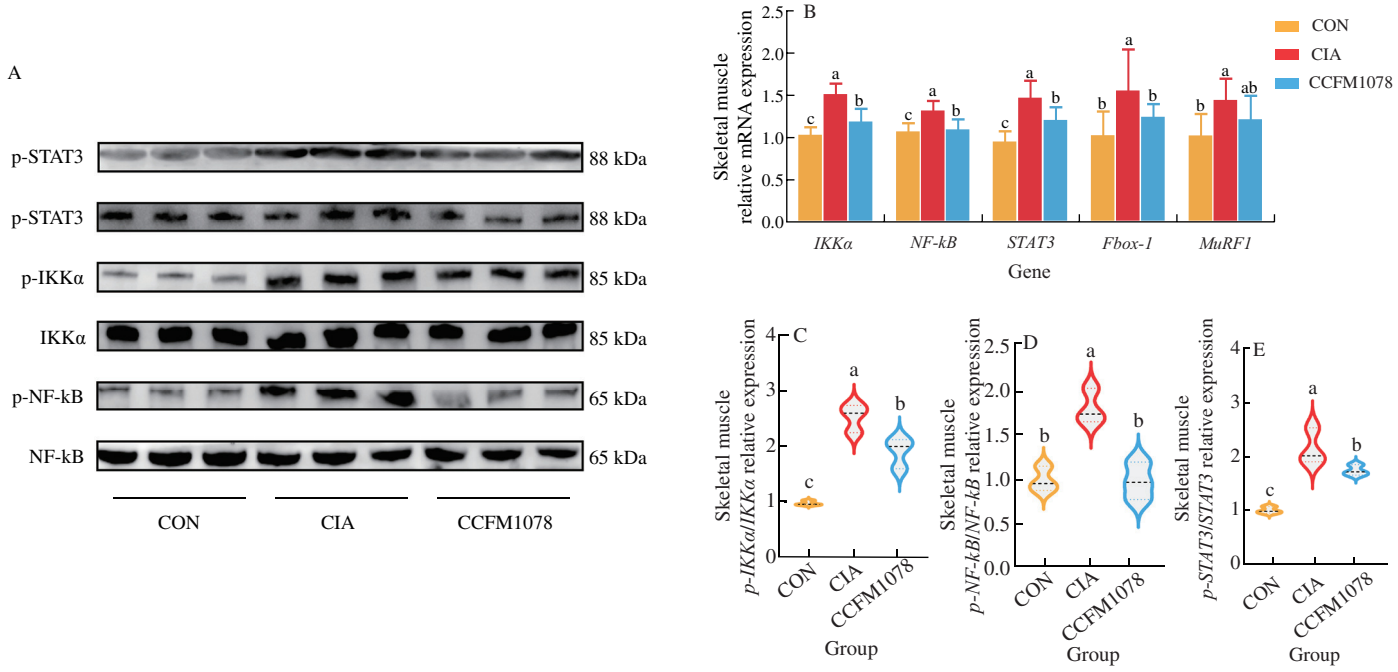

Fig. 6 Effects of *B. breve* CCFM1078 on NF-κB pathway in skeletal muscle of CIA rats. (A) p-STAT3, STAT3, p-IKKα, IKKα, p-NF-κB, NF-κB Western Blot strips, (B) skeletal muscle relative mRNA expression of *IKKα*, *NF-κB*, *STAT3*, *Fbox-1*, *MuRF1*, (C) skeletal muscle *p-IKKα/IKKα* relative expression, (D) skeletal muscle *p-NF-κB/NF-κB* relative expression, (E) skeletal muscle *p-STAT3/STAT3* relative expression. The completely different letters between each group represented significant differences, $P < 0.05$.

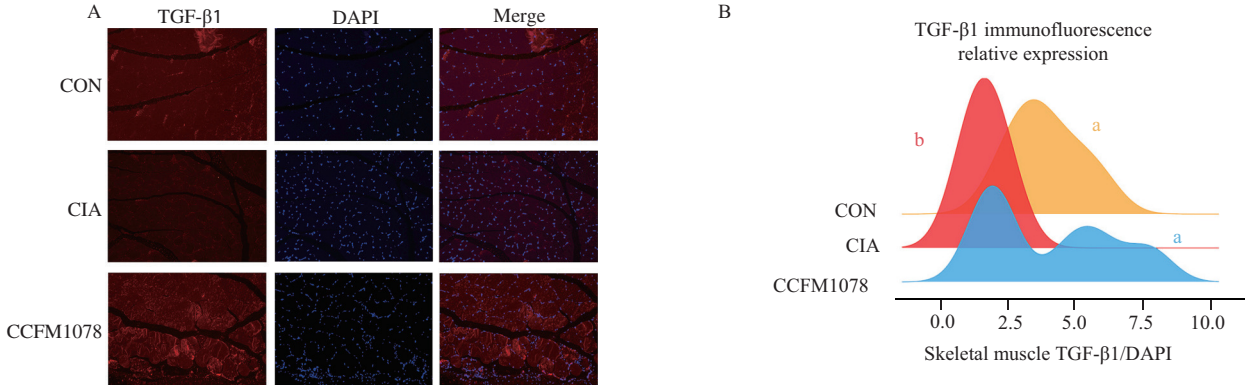

Fig. 7 Effects of *B. breve* CCFM1078 on IRS1/PI3K/Akt pathway in skeletal muscle of CIA rats. (A) Skeletal muscle TGF-β1 immunofluorescence, magnification: 200×. (B) Immunofluorescence relative expression of skeletal muscle TGF-β1 (TGF-β1/DAPI). (C) p-IRS1, IRS1, p-PI3K, PI3K, IGF1R, p-Akt, Akt, Glut4, MyoG, *β*-actin Western Blot strips. (D) TGF-β1 content in skeletal muscle. (E) Skeletal muscle Glut4 immunofluorescence, magnification: 200×. (F) Immunofluorescence relative expression of skeletal muscle Glut4 (Glut4/DAPI). (G) Skeletal muscle relative mRNA expression of *IGF1*, *TGF-β1*, *IRS1*, *PI3K*, *Akt*. (H) Skeletal muscle relative mRNA expression of *Glut4*, *MyoD*, *MyoG*, *GSK3β*. (I) Skeletal muscle relative non-coding RNA expression of H19, miR-29b-3p, (J) Skeletal muscle p-IRS1/IRS1 relative expression. (K) Skeletal muscle p-PI3K/PI3K relative expression, (L) Skeletal muscle IGF1R relative expression, (M) Skeletal muscle p-Akt/Akt relative expression. (N) Skeletal muscle Glut4 relative expression, (O) Skeletal muscle MyoG relative expression. The completely different letters between each group represented significant differences, $^{*}P < 0.05$; $^{**}P < 0.01$; ns, no significant.

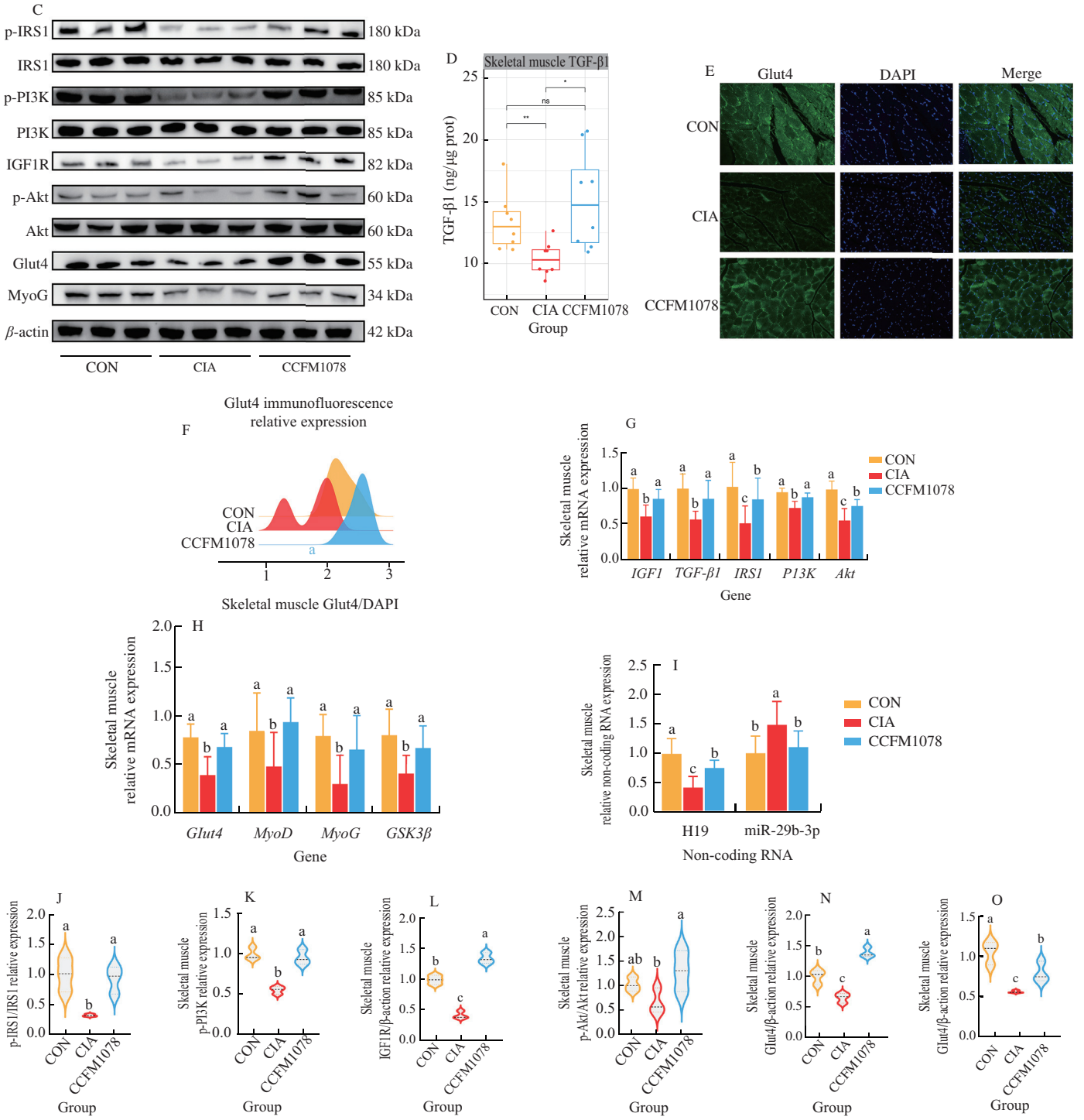

Fig. 7 (*Continued*)

3.8 RDA analysis of gut microbiota on various types of skeletal muscle indexes

The gut microbiota with significant differences contributed differently to RA indicators (RF, CRP, anti-CCP, Fig. 8A); skeletal muscle metabolic indicators (MG, lactate, Fig. 8B), skeletal muscle hormone indicators (11β-HSD1, 25(OH)D_3, Fig. 8C), skeletal muscle inflammation indicators (IL-6, TNF-α, IL-17, Fig. 8D), skeletal muscle atrophy indicators (MSTN, Fbox-1, Fig. 8E), and skeletal muscle differentiation indicators (TGF-β1, MyoD, Fig. 8F). In general, *Akkermansia*, *Bifidobacterium*, and *Turicibacter* positively contributed to the CON group and CCFM1078 group, whereas *Alistipes* and *Alloprevotella* positively contributed to the CIA group.

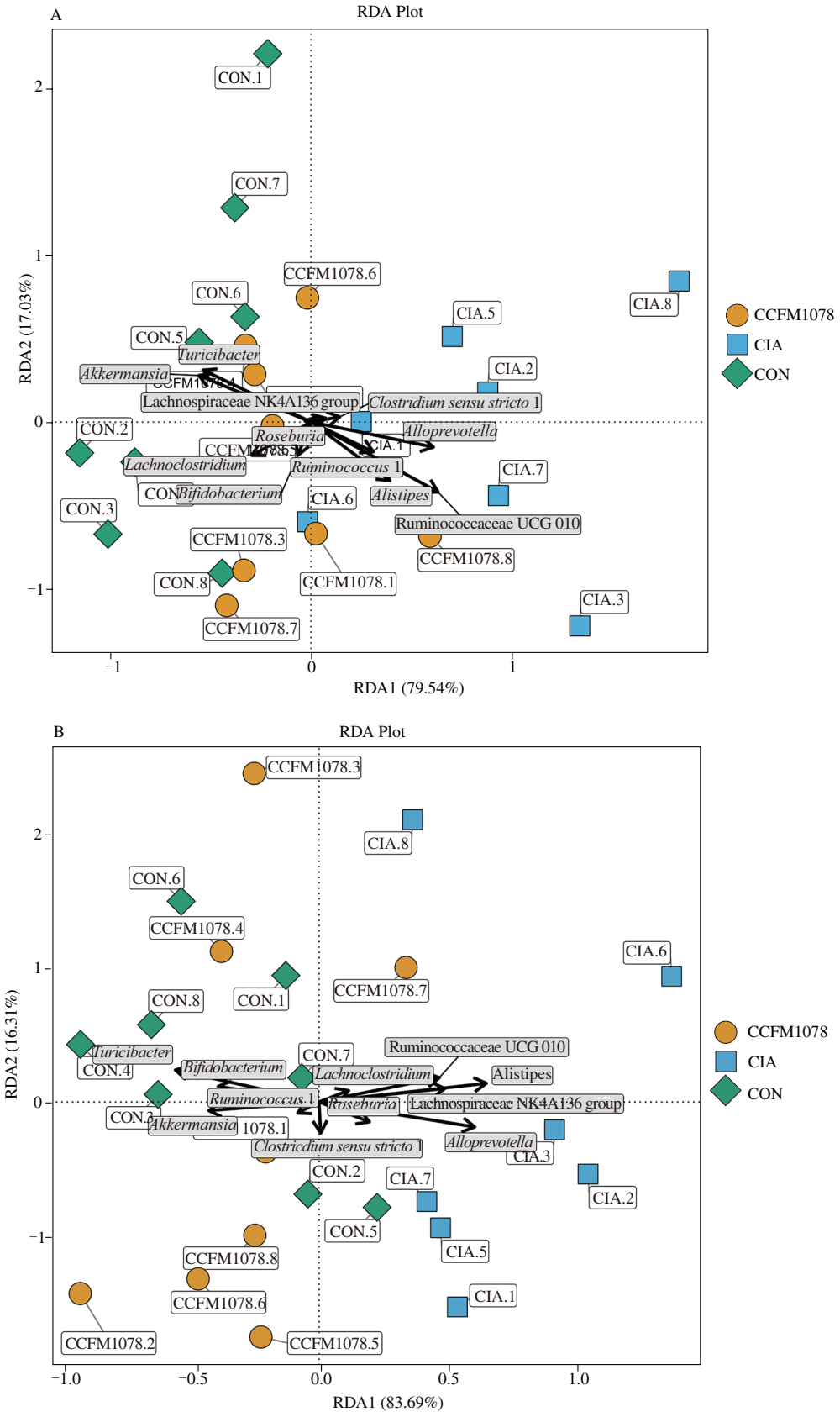

Fig. 8 RDA analysis of gut microbiota with significant differences. (A) Gut microbiota with rheumatoid arthritis indicators (RF, CRP, anti-CCP), (B) gut microbiota with skeletal muscle metabolic indicators (MG, lactate), (C) gut microbiota with skeletal muscle hormone indicators (11β-HSD1, 25(OH)D_3), (D) gut microbiota with skeletal muscle inflammation indicators (IL-6, TNF-α, IL-17), (E) gut microbiota with skeletal muscle atrophy indicators (MSTN, Fbox-1), (F) gut microbiota with skeletal muscle differentiation indicators (TGF-β1, MyoD).

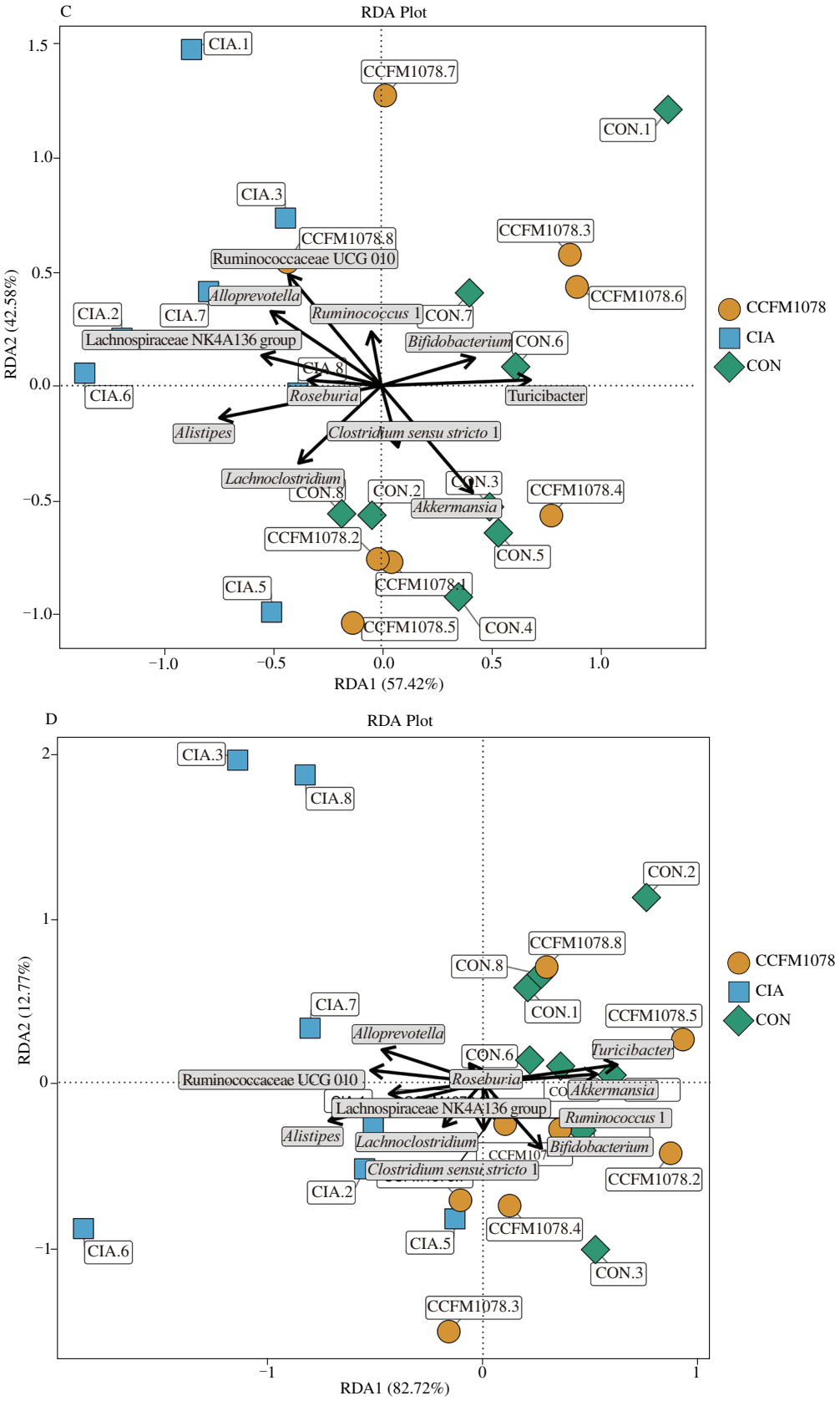

Fig. 8 (*Continued*)

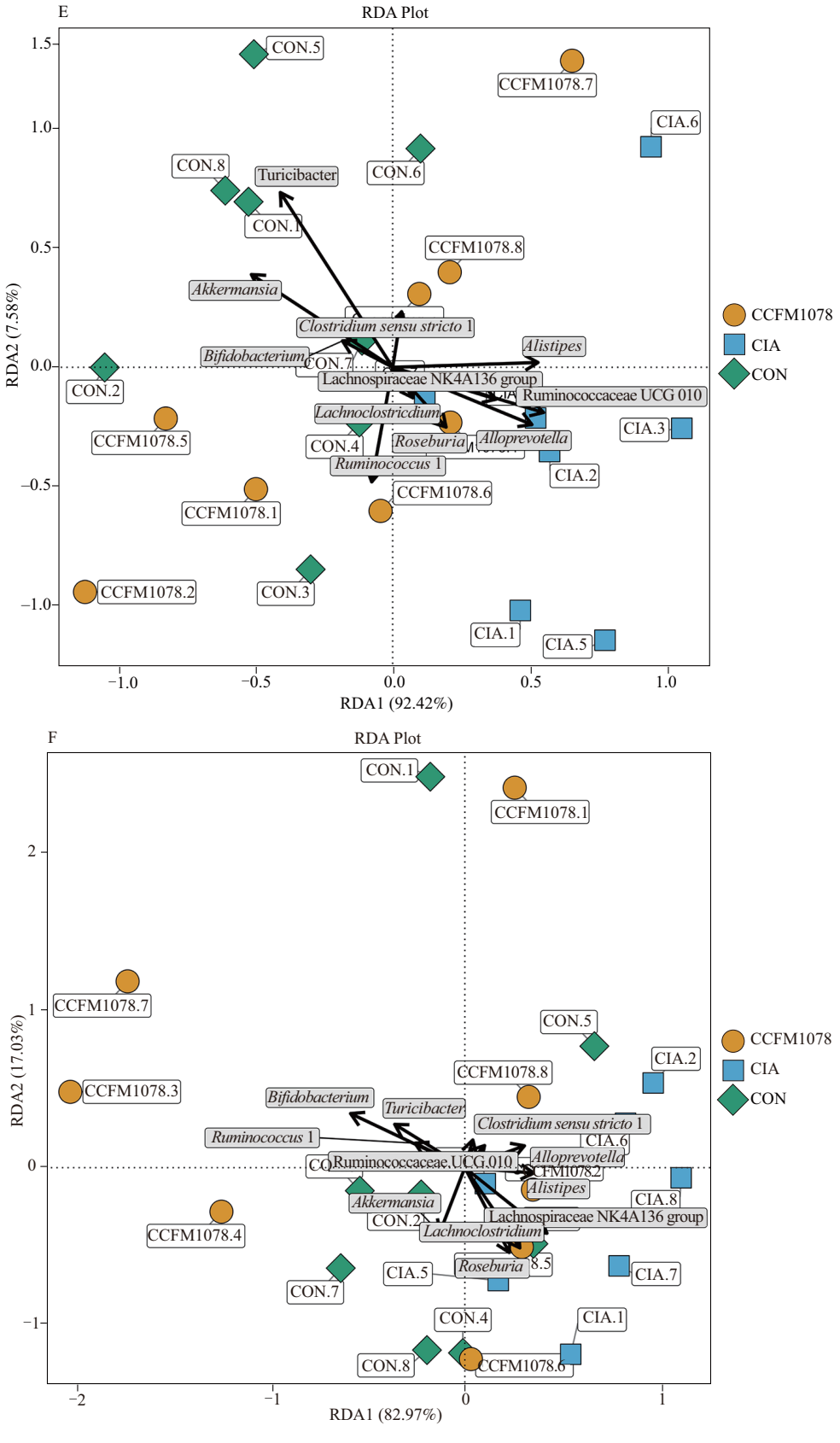

Fig. 8 (*Continued*)

4. Discussion

B. breve CCFM1078 can slow down the development speed and weaken the severity of RC. RF, CRP, and anti-CCP are comprehensive indicators for evaluating the development of RA[18]. RF is produced in peripheral lymph nodes, joint synovium, tonsil lymph follicles, and bone marrow, and it serves as a marker of autoimmune strength. CRP is a nonspecific inflammatory marker synthesized by the liver to protect the body during acute-phase reactions. Anti-CCP antibodies are spontaneously secreted by B lymphocytes in RA patients and have high specificity for RA[19]. Our results suggest that the development speed in the CCFM1078 group is slower than that in the CIA group, indicating that CCFM1078 may restrict the development of RA. The pull test in rats represented the functional performance of skeletal muscles. This means that CCFM1078 can not only restrict the development of RA but also improve the overall functional limitation of skeletal muscles to restrict the development of RC. The microscopic results of the knee joint and skeletal muscle were consistent with the macroscopic manifestations. The aggregation of monocytes represents the occurrence of inflammation. The extensive aggregation of monocytes in the synovial and trabecular regions of the CIA group rats represented a severe response to inflammation. Although inflammation existed in the CCFM1078 group, it was much weaker compared to the CIA group. The inflammatory changes in the CIA group also affected skeletal muscles, leading to protein breakdown of muscle fibers, muscle atrophy, thinning of the cartilage layer, and reduction of muscle collagen. The results indicated that CCFM1078 restricted the development of RC, consistent with the results of the pull test.

The changes in inflammation can affect muscle atrophy and differentiation. There have been studies showing that TNF-α and IL-6 affect the pathogenesis of RC[20]. TNF-α, as an inflammatory mediator, can not only inhibit the synthesis, metabolism, and differentiation of skeletal muscle, leading to increased protein degradation but also produce myolysis when exposed to TNF-α for a long time, activating the NF-κB pathway and damaging the structure and function of skeletal muscle[21]. Long-term exposure to IL-6 inhibits the IGF-1 signaling pathway and promotes muscle atrophy[22]. IL-17 may also further aggravate skeletal muscle damage and atrophy by inducing the release of cytokines and chemical mediators in muscle. The role of serum ALB in cachexia is associated with inflammatory response and immune function. The influence of inflammatory factors can lead to a decrease in serum ALB[23]. MG and lactate are important indicators for evaluating skeletal muscle metabolic function. MG is the main source of fuel in muscle cells. During muscle contraction, glycogen is broken down into glucose to supply energy to the muscles. When muscle glycogen stores are reduced or depleted, the muscles will not have enough energy to maintain normal contraction, resulting in muscle weakness and atrophy[24]. In addition, when muscle glycogen stores are inadequate, the body will break down muscle protein to produce energy, increasing the risk of muscle atrophy. The accumulation of lactate leads to a decrease in muscle pH, making the muscle environment more acidic and reducing muscle contractility and the occurrence of muscle fatigue. From a hormonal perspective, although CCFM1078 decreased 11β-HSD1 in skeletal muscle, but no significant with CIA group. 11β-HSD1 affects cortisol metabolism, thereby inhibiting protein synthesis and promoting protein degradation[25]. These changes may lead to muscle atrophy and functional decline. 25(OH)D_3 is a product of vitamin D and is involved in regulating muscle contraction and nerve conduction, improving muscle strength and endurance, and regulating calcium and phosphate balance[26]. Based on our results, *B. breve* CCFM1078 regulated muscle homeostasis by modulating 25(OH)D_3. MSTN regulates muscle development by inhibiting the proliferation and differentiation of muscle cells. It restricts the growth and repair of muscle fibers[27]. Fbox-1 also plays a role in promoting muscle protein breakdown in muscle atrophy. Fbox-1 is also called Atrogin1 or Fbxo32. Specifically, Fbox-1 interacts with another protein called MuRF1 to form a complex. This complex tag targets proteins through ubiquitination and then degrades them through proteasomes[28]. In contrast, MyoD regulates muscle cell differentiation and the generation of muscle fibers. An increase in MyoD in skeletal muscle promotes the proliferation and differentiation of muscle cells, thereby increasing muscle volume and strength[29]. In summary, from these indicators, we can regulate that *B. breve* CCFM1078 can affect the atrophy and differentiation of muscle cells by adjusting inflammatory factors, metabolism, hormones, and other relevant indicators in skeletal muscle, thus influencing the severity of muscle wasting.

The modulation of gut microbiota by *B. breve* CCFM1078 was an important factor in suppressing the onset of RC and RA. CCFM1078 had a relatively small regulatory effect on the alpha diversity of the fecal microbiota, which suggested that CCFM1078 may not improve gut health by regulating the richness and evenness of the microbial community. However, CCFM1078 can modulate the gut microbiota beta diversity, indicating its ability to alter the levels of different bacterial genera in the feces. Changes at the genus level of gut microbiota may be the reason behind the regulation of the RC process by *B. breve* CCFM1078. By analyzing the RDA plot and the relative abundance of differentially abundant microbial genera in the three groups, although there are slight differences in the results between the indicators. Overall, the increases of *Akkermansia*, *Bifidobacterium*, and *Turicibacter* led to results closer to the CON group and CCFM1078 group for each indicator. Conversely, the relative abundance increases of *Alistipes* and *Alloprevotella* resulted in indicators leaning towards the CIA group. This suggested that these differentially bacterial genera affect the development of RA and RC. *Akkermansia* has a regulatory role in the gut environment. It can not only adjust the balance of the gut microbiota and prevent the overgrowth of harmful bacteria but also regulate the thickness of the intestinal mucus layer, maintaining the integrity and function of the intestinal mucosa[30]. *Turicibacter* is a potentially beneficial genus, and the metabolic products of *Lycium barbarum* polysaccharides have been reported to improve the progression of CIA in rats by upregulating *Turicibacter*[31]. *Alistipes* is involved in inflammatory responses and is associated with certain diseases. The relative abundance of *Alistipes* significantly increased in the intestines of patients with inflammatory bowel diseases and obesity[32]. On the other hand, *Alistipes* shows lower relative abundance in the intestines of diabetic patients, and its quantity is related to blood glucose control[33]. These studies suggest that Alistipes may affect the occurrence of diseases by regulating intestinal inflammation and metabolic function. Previous study showed that the relative abundance of *Alloprevotella* was positively correlated with the level of RF or anti-cyclic citrullinated peptide antibodies, indicating that the increase of *Alloprevotella* may affect

the development of RA symptoms[34]. Regarding *Bifidobacterium*, the consumption of *B. breve* CCFM1078 can upregulate the Shannon index and increase the α-diversity of the bifidobacterial community. This result was contrary to our previous research. It was speculated that the differential regulation of bifidobacterial diversity in different batches of experimental animals by *B. breve* CCFM1078 may be partially attributed to the varying relative abundance of *Bifidobacterium* carried by the experimental animals themselves. Additionally, due to the relatively lower abundance of *Bifidobacterium* compared to the total bacterial population, the diversity of *Bifidobacterium* may be more susceptible to disturbance.

As shown in the RDA plot, the changes in gut microbiota regulated the levels of inflammatory factors, thereby regulating the NF-κB inflammatory pathway. Skeletal muscle cells, when stimulated by inflammatory factors such as TNF-α and IL-6, induce phosphorylation of IKKα, which further activates downstream phosphorylation of NF-κB[35]. When the NF-κB signaling pathway is activated, NF-κB translocates to the cell nucleus and binds with STAT3, thereby enhancing STAT3's transcription and translation ability[36]. Phosphorylated STAT3 also reactivates the expression of IL-17 and various inflammatory factors, leading to a vicious cycle[37]. This vicious cycle strengthens the transcription ability of Fbox-1 and MuRF1. Fbox-1 is believed to be involved in muscle protein degradation through the activation of proteasome formation via signaling transduction pathways, thereby triggering muscle tissue protein breakdown and muscle atrophy. MuRF1 can bind with Fbox-1 facilitating the selective degradation of proteins in the muscle. Moreover, MuRF1 is also involved in alterations of muscle structure, primarily manifested by inducing muscle fiber atrophy and reduction in fiber size[38].

B. breve CCFM1078 can also regulate the proliferation and differentiation of skeletal muscle through the IRS1/PI3K/Akt pathway. TGF-β1 and IGF1 are 2 important growth factors. Between them, TGF-β1 can promote the differentiation of myoblasts (undifferentiated muscle stem cells) into myofibers (differentiated muscle cells) during muscle differentiation. IGF-1, on the other hand, can enhance muscle protein synthesis, inhibit protein degradation, and promote muscle cell proliferation. It can achieve these effects by binding to the IGF-1 receptor on the cell membrane and triggering the IRS1/PI3K/Akt signaling pathway. After binding to its receptor, IGF-1 phosphorylates and activates IRS1. Activated IRS1 can bind to PI3K, further activating PI3K. PI3K can convert phosphatidylinositol 4,5-bisphosphate (PIP2) on the cell membrane into phosphatidylinositol 3,4,5-trisphosphate (PIP3). The PIP3 produced by this reaction recruits and activates Akt. In muscle cells, the activation of Akt can promote muscle protein synthesis, inhibit protein degradation, and enhance muscle cell differentiation[39]. Downstream Glut4, and GSK3β are involved in glucose transport and affects the synthesis of MG in muscles. High expression of MyoG is also believed to be involved in the differentiation of myoblasts into muscle fibers. Our results indicated that *B. breve* CCFM1078 can promote growth factors expression in skeletal muscles, then activating the expression of the IRS1/PI3K/Akt signaling pathway and regulating the expression of downstream Glut4 and MyoG, thereby influencing the progression of RC. The B.breve CCFM1078 may regulate the gut microbiota in a way that inhibits the NF-κB signaling pathway in skeletal muscles and activates the IRS1/PI3K/Akt signaling pathway, which could be a key mechanism for its regulatory effects on RC. It is worth noting that non-coding RNA may play a significant role upstream of TGF-β1, IGF1, and IRS1. Our previous studies have revealed that methionine restriction can regulate muscle atrophy and differentiation through the regulation of the lncRNA H19[40]. miR-29b-3p, as a downstream miRNA of H19, can decrease the expression of some genes encoding muscle structural proteins, such as MyoD, and MyoG, thereby exerting regulatory effects on skeletal muscle[41]. Therefore, it further expanded our investigation to detect the expression of H19 and miR-29b-3p in skeletal muscle. The results were consistent with our speculation that H19 and miR-29b-3p were involved in the regulation of skeletal muscle by *B. breve* CCFM1078. However, the exact effect *B. breve* CCFM1078 effects on the expression of non-coding RNA still needs further exploration, which will provide a new perspective and suggest that the regulation of gut microbiota by probiotics may influence the expression of non-coding RNA in skeletal muscle.

5. Conclusion

B. breve CCFM1078 can regulate the gut microbiota composition, thereby affecting the inflammation of joints and skeletal muscles, which led to the inhibition of the skeletal muscle inflammatory signaling pathway NF-κB and the activation of IRS1/PI3K/Akt pathway. *B. breve* CCFM1078 also reduced protein absorption, promoted skeletal muscle differentiation, and thereby slowed down the progression of RC. In this process, non-coding RNA may play a significant role. Our findings suggest that *B. breve* CCFM1078, as part of the dietary intervention for RC, may enhance the traditional therapeutic effects.

Conflict of interest

The authors declare no conflict of interest.

Acknowledgments

This research was supported by the National Natural Science Foundation of China (32021005), 111 project (BP0719028), and the Collaborative Innovation Center of Food Safety and Quality Control in Jiangsu Province.

Appendix A. Supplementary data

Supplementary data associated with this article can be found, in the online version, at http://doi.org/10.26599/ FSHW.2024.9250323.

References

[1] G.D. Summers, G.S. Metsios, A. Stavropoulos-Kalinoglou, et al., Rheumatoid cachexia and cardiovascular disease, Nature Reviews Rheumatology 6 (2010) 445-451. https://doi.org/10.1038/nrrheum.2010.105.

[2] L. Ångström, K. Hörnberg, B. Sundström, et al., Rheumatoid cachexia in early rheumatoid arthritis: prevalence and associated variables, Scandinavian Journal of Rheumatology 52 (2023) 10-16. https://doi.org/10.1080/03009742.2021.1973678.

[3] E. Efthymiou, M.G. Grammatikopoulou, K. Gkiouras, et al., Time to deal with rheumatoid cachexia: prevalence, diagnostic criteria, treatment effects and evidence for management, Mediterr. J. Rheumatol. 33 (2022) 271-290. https://doi.org/10.31138/mjr.33.3.271.

[4] R. de Sire, G. Rizzatti, F. Ingravalle, et al., Skeletal muscle-gut axis: emerging mechanisms of sarcopenia for intestinal and extra intestinal diseases, Minerva. Gastroenterol. Dietol. 64 (2018) 351-362. https://doi.org/10.23736/s1121-421x.18.02511-4.

[5] M. Jollet, M. Mariadassou, O. Rué, et al., Insight into the role of gut microbiota in duchenne muscular dystrophy: an age-related study in mdx mice, The American Journal of Pathology 194 (2024) 264-279. https://doi.org/10.1016/j.ajpath.2023.10.010.

[6] H.J. Kim, Y.J. Kim, Y.J. Kim, et al., Microbiota influences host exercise capacity via modulation of skeletal muscle glucose metabolism in mice, Experimental & Molecular Medicine 55 (2023) 1820-1830. https://doi.org/10.1038/s12276-023-01063-4.

[7] Y. Zhufeng, J. Xu, M. Miao, et al., Modification of intestinal microbiota dysbiosis by low-dose interleukin-2 in dermatomyositis: a post hoc analysis from a clinical trial study, Frontiers in Cellular and Infection Microbiology, 12 (2022) 757099.

[8] J. Suez, N. Zmora, E. Segal, et al., The pros, cons, and many unknowns of probiotics, Nature Medicine 25 (2019) 716-729. https://doi.org/10.1038/s41591-019-0439-x.

[9] M.C. Lee, C.S. Ho, Y.J. Hsu, et al., Live and heat-killed probiotic *Lactobacillus paracasei* PS23 accelerated the improvement and recovery of strength and damage biomarkers after exercise-induced muscle damage, Nutrients 14 (2022) 4563.

[10] S. Jabeen, J.I. Qazi, Oral administration of a locally isolated Lactobacillus rhamnosus (NR_113332.1) improves regeneration of extensor digitorum longus muscle in mice, Nutrition 114 (2023) 112110. https://doi.org/10.1016/j.nut.2023.112110.

[11] L.B. Bindels, R. Beck, O. Schakman, et al., Restoring specific Lactobacilli levels decreases inflammation and muscle atrophy markers in an acute leukemia mouse model, PLoS ONE 7 (2012) e37971. https://doi.org/10.1371/journal.pone.0037971.

[12] B. Li, M. Ding, X. Liu, et al., *Bifidobacterium breve* CCFM1078 alleviates collagen-induced arthritis in rats *via* modulating the gut microbiota and repairing the intestinal barrier damage, J. Agr. Food Chem. 70 (2022) 14665-14678. https://doi.org/10.1021/acs.jafc.2c04602.

[13] P.V.G. Alabarse, P.S. Lora, J.M.S. Silva, et al., Collagen-induced arthritis as an animal model of rheumatoid cachexia, J. Cachexia, Sarcopenia and Muscle 9 (2018) 603-612. https://doi.org/10.1002/jcsm.12280.

[14] Z. Fan, R.P. Ross, C. Stanton, et al., *Lactobacillus casei* CCFM1074 alleviates collagen-induced arthritis in rats via balancing Treg/Th17 and modulating the metabolites and gut microbiota, Frontiers in Immunology 12 (2021).

[15] M. Ding, Y. Zheng, F. Liu, et al., Lactation time influences the composition of *Bifidobacterium* and *Lactobacillus* at species level in human breast milk, Benef Microbes 13 (2022) 319-330. https://doi.org/10.3920/bm2021.0119.

[16] Y. Ge, B. Li, Y. Yang, et al., Oxidized pork induces disorders of glucose metabolism in mice, Molecular Nutrition & Food Research 65 (2021) 2000859. https://doi.org/10.1002/mnfr.202000859.

[17] Y. Ge, Y. Yang, Y. Jiang, et al., Oxidized pork induces hepatic steatosis by impairing thyroid hormone function in mice, Molecular Nutrition & Food Research 66 (2022) 2100602. https://doi.org/10.1002/mnfr.202100602.

[18] B. Li, B. Yang, X. Liu, et al., Microbiota-assisted therapy for systemic inflammatory arthritis: advances and mechanistic insights, Cellular and Molecular Life Sciences 79 (2022) 470. https://doi.org/10.1007/s00018-022-04498-6.

[19] M.V. Sokolova, G. Schett and U. Steffen, Autoantibodies in rheumatoid arthritis: historical background and novel findings, Clinical Reviews in Allergy & Immunology 63 (2022) 138-151. https://doi.org/10.1007/s12016-021-08890-1.

[20] J.M. Webster, L.J.A.P. Kempen, R.S. Hardy, et al., Inflammation and skeletal muscle wasting during cachexia, Frontiers in Physiology 11 (2020).

[21] D.C. Guttridge, M.W. Mayo, L.V. Madrid, et al., NF-κB-induced loss of myod messenger rna: possible role in muscle decay and cachexia, Science 289 (2000) 2363-2366. https://doi.org/10.1126/science.289.5488.2363.

[22] M. Torii, T. Itaya, H. Minamino, et al., Management of sarcopenia in patients with rheumatoid arthritis, Modern Rheumatology 33 (2023) 435-440. https://doi.org/10.1093/mr/roac095.

[23] A. Dolly, S.A. Pötgens, M.M. Thibaut, et al., Impairment of aryl hydrocarbon receptor signalling promotes hepatic disorders in cancer cachexia, Journal of Cachexia, Sarcopenia and Muscle 14 (2023) 1569-1582. https://doi.org/10.1002/jcsm.13246.

[24] K. Shiose, H. Takahashi, Y. Yamada, Muscle glycogen assessment and relationship with body hydration status: a narrative review, Nutrients 15 (2023).

[25] J.M. Webster, M.S. Sagmeister, C.G. Fenton, et al., Global deletion of 11β-HSD1 prevents muscle wasting associated with glucocorticoid therapy in polyarthritis, International Journal of Molecular Sciences (2021) 22.

[26] O. Czerwińska-Ledwig, D.H. Vesole, A. Piotrowska, et al., Effect of a 6-week cycle of nordic walking training on vitamin 25(OH)D_3, calcium-phosphate metabolism and muscle damage in multiple myeloma patients– randomized controlled trial, Journal of Clinical Medicine (2022) 11.

[27] K. Maeta, M. Farea, H. Nishio, et al., A novel splice variant of the human MSTN gene encodes a myostatin-specific myostatin inhibitor, Journal of Cachexia, Sarcopenia and Muscle 14 (2023) 2289-2300. https://doi.org/10.1002/jcsm.13314.

[28] A. Agrawal, R. Rathor, R. Kumar, et al., Role of altered proteostasis network in chronic hypobaric hypoxia induced skeletal muscle atrophy, PLoS ONE 13 (2018) e0204283. https://doi.org/10.1371/journal.pone.0204283.

[29] H. Zheng, F. Cheng, D. Guo, et al., Nanoenzyme-reinforced multifunctional scaffold based on ti3c2tx mxene nanosheets for promoting structure-functional skeletal muscle regeneration *via* electroactivity and microenvironment management, Nano Letters 23 (2023) 7379-7388. https://doi.org/10.1021/acs.nanolett.3c01784.

[30] A. Pellegrino, G. Coppola, F. Santopaolo, et al., Role of Akkermansia in human diseases: from causation to therapeutic properties, Nutrients, 2023, 15.

[31] Y. Liu, L. Liu, J. Luo, et al., Metabolites from specific intestinal bacteria *in vivo* fermenting *Lycium barbarum* polysaccharide improve collagenous arthritis in rats, International Journal of Biological Macromolecules 226 (2023) 1455-1467. https://doi.org/10.1016/j.ijbiomac.2022.11.257

[32] P. Yan, Y. Sun, J. Luo, et al., Integrating the serum proteomic and fecal metaproteomic to analyze the impacts of overweight/obesity on IBD: a pilot investigation, Clinical Proteomics 20 (2023) 6. https://doi.org/10.1186/s12014-023-09396-y

[33] R.A. Teixeira, C. Silva, A.C. Ferreira, et al., The association between gestational diabetes and the microbiome: a systematic review and meta-analysis. Microorganisms, 2023, 11.

[34] S. Cong, L. Wang, Y. Meng, et al., *Saussurea involucrata* oral liquid regulates gut microbiota and serum metabolism during alleviation of collagen-induced arthritis in rats, Phytotherapy Research 37 (2023) 1242-1259. https://doi.org/10.1002/ptr.7681.

[35] X. Chen, Y. Ji, R. Liu, et al., Mitochondrial dysfunction: roles in skeletal muscle atrophy, Journal of Translational Medicine 21 (2023) 503. https://doi.org/10.1186/s12967-023-04369-z.

[36] X. Yang, L. Xu, L. Yang, et al., Research progress of STAT3-based dual inhibitors for cancer therapy, Bioorganic & Medicinal Chemistry 91 (2023) 117382. https://doi.org/10.1016/j.bmc.2023.117382.

[37] J.Y. Chen, X.Y. Tian, S.S. Wei, et al., Magnolol as STAT3 inhibitor for treating multiple sclerosis by restricting Th17 cells, Phytomedicine 117 (2023) 154917. https://doi.org/10.1016/j.phymed.2023.154917.

[38] J.P. Gumucio, C.L. Mendias, Atrogin-1, MuRF-1, and sarcopenia, Endocrine 43 (2013) 12-21. https://doi.org/10.1007/s12020-012-9751-7.

[39] A. Banerjee and D.C. Guttridge, Mechanisms for maintaining muscle, Current Opinion in Supportive and Palliative Care 6 (2012).

[40] C. Feng, Y. Jiang, G. Wu, et al., Dietary methionine restriction improves gastrocnemius muscle glucose metabolism through improved insulin secretion and H19/IRS-1/Akt pathway in middle-aged mice, J. Agricultural and Food Chemistry 71 (2023) 5655-5666. https://doi.org/10.1021/acs.jafc.2c08373.

[41] Q. Liu, W. Yuan, Y. Yan, et al., Identification of a novel small-molecule inhibitor of miR-29b attenuates muscle atrophy, Molecular Therapy - Nucleic Acids 31 (2023) 527-540. https://doi.org/10.1016/j.omtn.2023.02.003.